Improving the Catalytic Activity of a Thermophilic Enzyme at Low Temperatures[†]

Astrid Merz,[‡] Muh-ching Yee,[§] Halina Szadkowski,[‡] Günter Pappenberger,[‡] Andreas Crameri,[∥] Willem P. C. Stemmer,[⊥] Charles Yanofsky,[§] and Kasper Kirschner*[,‡]

Department of Biophysical Chemistry, Biozentrum, Klingelbergstrasse 70, 4056 Basel, Switzerland, Department of Biological Sciences, Stanford University, Stanford, California 94305-5020, Department of Pharmacology, Biozentrum, Klingelbergstrasse 70, 4056 Basel, Switzerland, and Maxygen, Inc., 515 Galveston Drive, Redwood City, California 94063

Received October 7, 1999; Revised Manuscript Received November 18, 1999

ABSTRACT: Enzymes from thermophilic organisms often are barely active at low temperatures. To obtain a better understanding of this sluggishness, we used DNA shuffling to mutagenize the *trpC* gene, which encodes indoleglycerol phosphate synthase, from the hyperthermophile *Sulfolobus solfataricus*. Mutants producing more active protein variants were selected by genetic complementation of an *Escherichia coli* mutant bearing a *trpC* deletion. Single amino acid changes and combinations of these changes improved growth appreciably. Five singly and doubly altered protein variants with changes at the N- and C-termini, or at the phosphate binding site, were purified and characterized with regard to their kinetics of enzymatic catalysis, product binding, cleavage by trypsin, and inactivation by heat. Turnover numbers of the purified variant proteins correlated with the corresponding growth rates, showing that the turnover number was the selected trait. Although the affinities for both the substrate and the product decreased appreciably in most protein variants, these defects were offset by the accumulation of high levels of the enzyme's substrate. Rapid mixing of the product indoleglycerol phosphate with the parental enzyme revealed that the enzyme's turnover number at low temperatures is limited by the dissociation of the enzyme−product complex. In contrast, representative protein variants bind and release the product far more rapidly, shifting the bottleneck to the preceding chemical step. The turnover number of the parental enzyme increases with temperature, suggesting that its structural rigidity is responsible for its poor catalytic activity at low temperatures. In support of this interpretation, the rate of trypsinolysis or of thermal denaturation is accelerated significantly in the activated protein variants.

It is important to understand the relationship between the stability of an enzyme and its catalytic function. Many X-ray structures of thermostable enzymes have been determined in recent years and compared to the structures of their mesophilic counterparts in an effort to explain the molecular bases of thermostability (*1*, *2*). Generally, the overall structures of orthologous thermophilic and mesophilic proteins were found to be quite similar. The thermostability of monomeric proteins seems to be achieved by an individual combination of different strategies, such as optimized packing of the hydrophobic core and an increased level of burial of the hydrophobic surface area, improved stabilization of secondary structural elements, an increased number of hydrogen bonds and salt bridges (often in clusters) at the protein surface, and shortened surface loops and fixed chain termini.

Thermostable enzymes are generally barely active at room temperature, but are as active at their optimal growth temperatures ["corresponding states" (*1*)] as their thermolabile counterparts from mesophiles (*3*). Because the active site structures are superimposable and the catalytic residues conserved, it is generally assumed that both thermolabile and thermostable enzymes share the same catalytic mechanism. It is unlikely that cold denaturation is responsible for this phenomenon, because X-ray structures of thermostable proteins obtained from crystals grown at low temperatures show natively folded proteins. Recent studies (*4*−*6*) suggest that it might be the reduced flexibility of thermostable enzymes that impairs their catalytic activity at low temperatures.

The aim of this study was to isolate variants of the monomeric enzyme indoleglycerol phosphate synthase (IGPS)[1] from *Sulfolobus solfataricus* that increase the activity of this hyperthermostable enzyme at 37 °C. The positions of amino acid substitutions should identify structural elements that are responsible for the functional sluggishness of the parental protein. *S. solfataricus* is a hyperthermophilic archaeon that grows in hot, acidic, and sulfurous volcanic pools. IGPS from this organism (sIGPS) is stable and active at 85 °C (*7*), where

[†] This work was supported by grants from the Swiss National Science Foundation to K.K. (31-45855.95) and the United States Public Health Service to C.Y. (GM09738).

* To whom correspondence should be addressed: Department of Biophysical Chemistry, Biozentrum, Klingelbergstrasse 70, CH-4056 Basel, Switzerland. Phone: 0041-61-267 21 80. Fax: 0041-61-267 21 89. E-mail: Kasper.Kirschner@unibas.ch.

[‡] Department of Biophysical Chemistry, Biozentrum.

[§] Stanford University.

[∥] Department of Pharmacology, Biozentrum.

[⊥] Maxygen, Inc.

[1] Abbreviations: IGP, indoleglycerol phosphate; IGPS, IGP synthase; sIGPS, IGPS from *S. solfataricus*; eIGPS, IGPS from *E. coli*; tIGPS, IGPS from *Thermotoga maritima*; PRAI, phosphoribosyl anthranilate isomerase; ePRAI, PRAI from *E. coli*; *trpC*, gene encoding IGPS; *trpF*, gene encoding PRAI; CdRP, 1-(*o*-carboxyphenylamino)-1-deoxyribulose 5-phosphate; HEPPS, 4-(2-hydroxyethyl)-1-piperazinepropanesulfonic acid.

10.1021/bi992333i CCC: $19.00
Published on Web 01/11/2000

S. solfataricus grows optimally, but relatively inactive at 37 °C compared to its mesophilic counterpart from *Escherichia coli* (eIGPS). sIGPS is a good model enzyme to study, since the crystal structures of both sIGPS (*7*) and eIGPS (*8*) are known. They share the TIM-barrel fold with a root-mean-square deviation of 1.73 Å for 239 equivalent superimposed Cα atoms (*7*).

Here we show that it is possible to generate sIGPS variants with single and double amino acid substitutions that improve the catalytic activity of sIGPS at 37 °C. The selected trait of the sIGPS variants was a greater turnover number, which occurred at a cost of greatly decreasing the affinity for both the substrate and product. Thus, substrate turnover by the parental protein at low temperatures is limited by product release. Single-residue changes can accelerate product release, and combining two changes can accelerate catalysis. These changes correlate with increased flexibility of the protein.

MATERIALS AND METHODS

Strains. E. coli strain JMB9 r^-m^+ Δ*trpC*, which was used to select active variants of eIGPS after saturation mutagenesis (*9*), could be transformed only with low efficiency. The Δ*trpC* deletion was therefore transduced into W3110 *tnaA2 hsdR2, zji-202*::Tn*10*, which has a much better transformation efficiency, yielding W3110 Δ*trpC tnaA*2 *hsdR2, zji-202*::Tn*10*. It was used as a recipient in experiments designed to detect sIGPS-bearing plasmids that confer ability to grow in the absence of added tryptophan. The chromosomal *trpC* region deletion present in these strains leaves the *trpF* coding region intact and functional. Thus, the recipient is $trpC^-$ $trpF^+$ and would require only IGPS function to grow in the absence of a tryptophan supplement.

Plasmids. The parental plasmid pDS SS-1 (*7*) contains the *trpC* gene of *S. solfataricus* encoding wild-type sIGPS inserted into the *Sph*I and *Pst*I restriction sites of the expression vector pDS56/RBSII (*10*). In this vector, the *trpC* gene is transcribed from a modified T5 promoter that is regulated by the *lac* operator. The initial group of sIGPS variants was isolated in strain W3110 Δ*trpC tnaA2 hsdR2, zji-202*::Tn*10* containing plasmid pMS421, which carries the *lac* repressor allele $lacI^q$. This strain was transformed with a library of shuffled *trpC* genes inserted into pDS SS-1 in place of the parental *trpC* gene. We found this system to be unsuitable, because the *lac* operator of pDS SS-1 underwent fairly frequent spontaneous mutations, resulting in a loss of repressor binding. To reduce the likelihood of recovering mutations outside of *trpC*, and to avoid the necessity of using two plasmids in the selection procedure, we replaced the *lac* promoter of pDS SS-1 with a truncated derivative of the tryptophanase (*tna*) operon promoter. The region of nucleotides −30 to −10 of the *E. coli tna* operon promoter was substituted for the *Xho*I to *Eco*RI region of the pDS SS-1, replacing the *lac* promoter/operator. This plasmid, designated pMCY1, and its shuffled derivatives, were transformed into strain W3110 Δ*trpC tnaA2 hsdR2, zji-202*::Tn*10* to select for faster growers. Some altered *trpC* genes initially isolated in pDS SS-1 were subcloned into pMCY1 for analysis.

DNA Shuffling Procedure. The *trpC* gene from *S. solfataricus* was initially amplified using Vent polymerase, a high-fidelity proofreading polymerase from New England Biolabs. The amplified DNA was digested with DNase I in the presence of Mg^{2+} to obtain fragments that were 50−200 bp long. The DNase-treated DNA sample was subjected to a primerless polymerase chain reaction (PCR; *11*, *12*) using equal amounts of *Taq* (LifeSciences) and *Pfu* (Stratagene) polymerases to reassemble the *trpC* gene. The combination of *Taq* and *Pfu* polymerases (*13*) was used to reduce the mutation rate compared to those in earlier procedures (*11*).

Amplification Procedures. The reassembled DNA pool was used as a template in PCR with three primer pairs. The entire coding region was amplified using outside 5′- and outside 3′-primers and subcloned into pMCY1 for transformation and selection. The 5′-half of the coding region was amplified using one outside 5′-primer and one internal 3′-primer. The 3′-half of the coding region was amplified using one outside 3′-primer and one internal 5′-primer. The two internal primers flank a unique *Nsi*I restriction site in the middle of *trpC*. Thus, the product of the upstream outside primer and its matching internal primer encodes the N-terminal half of sIGPS and has an *Sph*I site at the 5′-end and an *Nsi*I site at the 3′-end. This fragment can then be recloned into the corresponding restriction sites of plasmid pMCY1. Likewise, the product of the downstream primer and its matching internal primer encodes the C-terminal half of sIGPS and has an *Nsi*I site at the 5′-end and a *Pst*I site at the 3′-end. Cloning the shuffled pool in two halves allowed rapid location and identification of single changes that result in faster growth. The same reassembled pool was the template in several amplification procedures, using the three different primer pairs; a different set of mutants was isolated in each experiment.

Hydroxylamine Mutagenesis. The *trpC* gene of pMCY1 was subjected to hydroxylamine mutagenesis as described by Davis et al. (*14*). Subsequently, the *trpC* inserts were cut out using the restriction enzymes *Eco*RI and *Pst*I and subcloned into the corresponding sites of an unmutated pMCY1 vector. Amino acid replacements S58F, G59R, S70L, and S181A/D165A were introduced using this approach.

Recombination of Mutations. Selected single mutants were combined with one another using the unique *Nsi*I site in the middle of the gene (*15*) to test the effects of combining single alterations. Double mutants P2S/G212E and P2S/F246S were prepared in this way.

Selection Procedure. Recloned shuffled genes were transformed into strain W3110 Δ*trpC tnaA2 hsdR2, zji-202*::Tn*10*, or its pMS421-containing derivative, and plated on minimal VB (*16*) agar plates supplemented with 0.2% glucose, 0.05 μg/mL L-tryptophan, and 50 μg/mL carbenicillin. Colonies that grew after incubation for 1−2 days at 37 °C were restreaked, their plasmids subcloned and retransformed, and the transformants replated, to confirm that alteration of the *trpC* coding region was responsible for faster growth. The subcloned part of the gene was then sequenced to determine the mutational change(s). The frequency of transformants with shuffled DNA that grew on the test minimal agar plates was ca. $1/10^4$. The frequency observed with a culture transformed with the untreated parental vector was ca. $1/10^6$.

Growth Curves and Accumulation of CdRP. Growth of cultures in minimal medium was assessed using W3110 Δ*trpC tnaA2 hsdR2, zji-202*::Tn*10* containing pMCY1-bearing parental or mutant *trpC* genes. Cultures were grown

with shaking at 37 °C in flasks containing liquid minimal medium (*16*) supplemented with 0.2% glucose, 0.05% acid-hydrolyzed casein, and 100 μg/mL ampicillin. After growth for 6 and 18 h (overnight), a sample of each culture was removed and assayed for cell density and the accumulation of CdRP. The cell density was determined using a Klett Colorimeter (66 filter). CdRP accumulation was determined qualitatively in each culture filtrate using a tetrazolium color test (*17*), by removing 1 mL of culture and adding 0.1 mL of 1 M NaOH and then 0.1 mL of a solution of 0.5% triphenyltetrazolium in chloroform. A red color develops within 1 min that is proportional to the amount of CdR and CdRP that has accumulated.

Activity Measurements. For determination of the relative specific activities of extracts of cultures containing the sIGPS variants, *E. coli* W3110 Δ*trpEA2 tnaA2 hsdR2* (*18*) was transformed with pMCY1 plasmids bearing the respective mutant *trpC* genes. All cultures except the control *E. coli* strain W3110 were grown overnight at 37 °C in liquid minimal medium supplemented with 0.2% glucose, 0.05% acid-hydrolyzed casein, 20 μg/mL L-tryptophan, and 100 μg/mL ampicillin. The control was grown in minimal medium without tryptophan or ampicillin. Cells were harvested by centrifugation, washed, suspended in 0.1 M Tris chloride (pH 7.8), and disrupted by sonication. The homogenates were centrifuged, and the activity in the supernatants was determined by measuring the extent of IGP formation using the periodate oxidation assay procedure (*19*). The substrate CdRP was produced chemically. In this procedure, aliquots of cell extracts were incubated in 0.25 mL reaction volumes containing 0.16 μmol of CdRP, 0.1 M Tris chloride (pH 7.8), 1 mM EDTA, and 1 mM DTT. Reactions were terminated by chilling and the addition of 0.05 mL of 2 M sodium acetate buffer (pH 5.0). The protein concentration was determined according to the method of Lowry (*20*).

Protein Purification. Production of sIGPS and its variants G212E, F246S, P2S/F246S, and P2S/G212E was carried out in W3110 *tna A2* Δ*trpC hsdR2*, *zji-202*::Tn*10* cells that had been transformed with two plasmids, pMS421 (encoding the *lac* repressor) and either pDS G212E, pDS F246S, pDS P2S/G212E, or pDS P2S/F246S (derivatives of the pDS SS-1 vector encoding the respective sIGPS variants). Production of the protein variant P2S was carried out in JMB9 r^-m^+ Δ*trpC* cells (*9*) that had been transformed with the plasmids pDS P2S and pDmI,1, encoding the mutant protein P2S and the *lac* repressor, respectively. Cells were grown at 37 °C in LB medium, supplemented with 50 μg/mL carbenicillin and 50 μg/mL spectinomycin (variants G212E, F246S, P2S/F246S, and P2S/G212E) or 0.1 mg/mL ampicillin and 25 μg/mL kanamycin (variant P2S). Overexpression was induced when the cells had reached an optical density at 600 nm of 0.6, by adding IPTG to a final concentration of 1 mM, and growth was continued for an additional 6 h. About 1.2−2.6 g of cells (wet weight) was obtained per liter of culture. Purification of all proteins was performed essentially as described for wild-type sIGPS (*7*) with minor modifications; e.g., DNA precipitation by protamine sulfate was omitted. The length and temperature of the heat step were adapted to the individual proteins: 15 min at 75 °C for variants F246S and G212E, 10 min at 68 °C for sIGPS P2S/G212E, and 10 min at 70 °C for sIGPS P2S. No heat treatment was used with sIGPS P2S/F246S. All purified proteins were found to be greater than 98% pure as judged by SDS−PAGE. Overall, 0.5−3 mg of protein was obtained per gram of wet cell paste.

Enzyme Kinetics. Steady-state parameters were determined at 37 °C in 0.05 M HEPPS buffer (pH 7.5) and 4 mM EDTA as described previously (*21*). The substrate CdRP used in these analyses was produced enzymatically (*22*). An independent estimate of the Michaelis constant K_M was first obtained by measuring initial velocities at various substrate concentrations, followed by direct-linear plot analysis (*23*). Complete progress curves were then recorded and fitted to the integrated Michaelis−Menten equation (*22*, *24*), using the preliminary K_M value to initiate the iteration. All protein concentrations were determined by using their extinction coefficients at 280 nm calculated from their content of tryptophan and tyrosine (*25*): $\epsilon_{280} = 20\,400\ M^{-1}\ cm^{-1}$; $A^{0.1\%}_{280} = 0.71\ cm^2\ mg^{-1}$.

Ligand Binding. The concentration of IGP was determined spectrophotometrically [$\epsilon_{278} = 5.4\ mM^{-1}\ cm^{-1}$ (*26*)]. Fluorescence titrations were performed at 37 °C in 0.05 M HEPPS buffer (pH 7.5) and 4 mM EDTA, using the Hitachi F-4500 fluorescence spectrophotometer. Small aliquots of an IGP stock solution were added with stirring to the protein solution (1.1 μM), allowing the mixture to equilibrate for 1 min before measuring fluorescence. Fluorescence was excited at 295 nm and recorded at 330 nm for 2 min to improve the signal-to-noise ratio by averaging. The ligand was also added to buffer in a separate titration to generate the baseline.

Kinetics of Ligand Binding. Stopped-flow studies were performed at 37 °C in 0.05 M HEPPS buffer (pH 7.5) and 4 mM EDTA, using the Applied Photophysics SX.18 MV stopped-flow reaction analyzer. Protein solutions at a constant concentration (0.2 μM) and ligand solutions were mixed in a 1:1 ratio; the final IGP concentration was varied between 0.5 and 5.5 μM (for sIGPS) and between 0.5 and 2 μM (for the F246S variant). Fluorescence was excited at 295 nm, and the increase in fluorescence emission was recorded using a 320 nm cutoff filter. The recording time of transients was adjusted to be in the range of $5/k_{obs}$ and the instrument response time not to exceed $0.01/k_{obs}$. Ten to twenty-four traces were recorded and averaged at each ligand concentration.

Limited Proteolysis. Protein (0.3 mg/mL) was incubated with 0.03 mg of trypsin/mL at 25 °C in 0.1 M Tris acetate (pH 7.8) and 2.5 mM EDTA, without and with a concentration of IGP that gives 90% saturation of the enzyme, based on the known value of the particular equilibrium dissociation constant ($K_P = K_d$). Samples were withdrawn after incubation for 1, 2, 5, 10, 20, 60, and 120 min and 20 h. The samples were mixed immediately with SDS sample buffer, heated to 100 °C for 5 min, electrophoresed on 12.5% SDS−polyacrylamide gels, and stained with Coomassie blue. Half-lives were estimated visually. The monomeric ePRAI domain (*22*) is cleaved by trypsin to small peptides at the same rate, regardless of whether 36 μM IGP was present or absent.

Kinetics of Irreversible Heat Inactivation. The protein stock solutions [20 μM in 0.05 M potassium phosphate buffer (pH 7.5), 2 mM EDTA, and 300 mM NaCl] were diluted to a final concentration of 1 μM by injection into degassed 0.05 M potassium phosphate buffer (pH 7.5) and 2 mM EDTA that was prewarmed to 87 °C and overlaid with mineral oil to prevent evaporation. Samples were taken after different time intervals and immediately chilled on ice. The residual

enzymatic activity was determined by recording initial reaction velocities at 37 °C in 0.05 M HEPPS buffer (pH 7.5) and 4 mM EDTA (*21*). The loss of activity with time was fitted to a monoexponential decay.

RESULTS AND DISCUSSION

Isolation of Activated Variants of sIGPS. The s*trpC* gene of *S. solfataricus* (encoding the enzyme sIGPS) was subjected to DNA shuffling (*11*, *12*) so sIGPS variants with improved catalytic activity at 37 °C could be obtained. Two different s*trpC*-containing plasmids were used, pDS SS-1 and pMCY1 (see Materials and Methods). Clones of the desired phenotype were selected by genetic complementation of an *E. coli* host strain with a deletion of the 5′-terminal *trpC* portion of the chromosomal bifunctional *trpC(F)* gene (Δ*trpC*), which is therefore incapable of growing on minimal medium lacking tryptophan (*9*). This deletion allows the production of the monofunctional, monomeric phosphoribosyl anthranilate isomerase domain [ePRAI (*22*)] and does not otherwise affect regulation of expression of the remainder of the *trp* operon. Pools of plasmids bearing mutant s*trpC* genes were transformed into Δ*trpC* recipient cells, and the transformed cells were plated on minimal agar plates. Colonies that grew faster than those obtained with controls containing the parental s*trpC* gene were assumed to be producing sIGPS variants that were more active than the parental protein at low temperatures. Plasmid DNA was isolated from each faster growing colony, and the mutated s*trpC* gene was sequenced to determine nucleotide and inferred amino acid changes.

DNA shuffling was used initially because we believed that it might be necessary to introduce multiple changes in the protein to obtain accelerated growth on minimal agar at 37 °C. Since the first few rounds of mutagenesis and screening revealed that single-amino acid changes were sufficient to allow improved growth under our selective conditions, we modified the shuffling and amplification procedure so that functional singly altered proteins were more likely to be recovered. The sequences of our mutant clones revealed that there were generally zero to two silent nucleotide changes in addition to each single-nucleotide change that was responsible for good growth. Each of the amino acid replacements we observed was due to a single-nucleotide change. Since the first round of DNA shuffling yielded functional proteins with single-residue replacements, we also mutagenized the s*trpC* gene with hydroxylamine to obtain more singly altered s*trpC* genes.

Location of Amino Acid Substitutions. The predicted amino acid substitutions in the mutant proteins are presented in Figure 1A along with a sequence alignment that is based on the known X-ray structures of sIGPS (*7*, *27*) and eIGPS (*8*). Most substitutions are clustered in loops connecting β-strands with α-helices ($\beta_i\alpha_i$) and in α-helices (α_i), identifying regions that appear to be important for activating sIGPS at low temperatures. However, a continuous segment of the protein, comprising about 40% of the sequence ($\beta_2-\beta_5$), has no substitution.

Seven out of 18 single-amino acid changes are at positions that are either invariant or conserved (Figure 1A), but most substitutions are disruptive, meaning that hydrophilic side chains replace hydrophobic ones, or vice versa. P2QΔ(4−28) is an unexpected variant, in which the entire helix α_0 is deleted. Among the two conservative substitutions (K53R and R54H), K53 is an invariant residue that forms a salt bridge to the substrate phosphate. The substitution of the equivalent residue K55 in eIGPS-PRAI with serine reduces the k_{cat} value 20-fold and increases K_M about 2000-fold (*28*), suggesting that it is a catalytically essential residue. Since K53R activates rather than inactivates sIGPS at 37 °C, it is not clear why K53 is invariant in all known IGPS sequences. However, since R53 is positively charged, it presumably can still interact with the substrate phosphate. Loop $\beta_1\alpha_1$ at the active site contains six out of 18 single substitutions, and the S58F change involves a highly conserved residue and G59R an invariant residue. S60 is the residue in eIGPS that is equivalent to S58, and the change S60A increases k_{cat} 2-fold and K_M 5-fold (*9*), an indication of its importance in catalysis. Nevertheless, the specific roles of S58 and G59 in the catalytic mechanism of sIGPS are still unknown.

The following subset of single-substitution variants was picked for further analysis: P2S, G212E, L236Q, M237T, and F246S. Figure 1B presents the ribbon diagram of sIGPS viewed from the side. The first 48 N-terminal residues are an extension of the $(\beta\alpha)_8$-barrel, with helix α_0 at the top and helix α_{00} at the bottom of the central, parallel β-barrel. It is seen that the substitutions P2S, G212E, L236Q, and M237T are located mainly on the N-terminal face of the β-barrel. The active site is identified by catalytically important residues E51, K53, K110, E159, and N180 (*9*), and by the bound phosphate ion, which presumably occupies the position of the phosphate moieties of the substrate and product (*7*). In contrast, F246S is located at the end of C-terminal helix α_8. The s*trpC* gene possesses a unique *Nsi*I restriction site in the middle of the DNA sequence (*15*), corresponding to the codons of A125 and Y126 (Figure 1A). The presence of this site allows mutational changes in the 5′- and 3′-terminal halves of the gene to be readily combined in vitro, to determine whether the individual contributions to increased activity are additive.

Growth Rates and Accumulation of CdRP. Freshly prepared and purified transformants containing each mutant gene producing a more active sIGPS variant were grown in liquid minimal medium to obtain a semiquantitative measure of growth rates. Growth curves obtained with strains carrying the selected set of altered *trpC* plasmids are shown in Figure 2. G212E was the fastest growing single-mutant variant, followed by L236Q, F246S, and M237T. P2QΔ(4−28) grew as rapidly as M237T (data not shown). Strains with single-mutant plasmids K53R, R54H, D183Y, E192A, and Q194R supported growth rates that were between those of strains with plasmids P2S and M237T (data not shown). None of the remaining single-site variants indicated in Figure 1A grew as well as F246S or G212E in streaks on minimal agar lacking tryptophan, and were not examined further.

The P2S substitution, by itself, had the smallest effect on growth rate. However, when P2S was combined with single substitutions between loop $\beta_7\alpha_7$ and the C-terminus (Figure 1A), these doubly altered variants supported even faster colony growth rates than either parent alone (Figure 2). This cooperative effect was also observed when the deletion P2QΔ(4−28) was combined with several single-site variants (data not shown). P2S with G212E (P2S/G212E) supported growth equivalent to the maximum growth rate observed in the presence of excess added tryptophan (see the G212E +

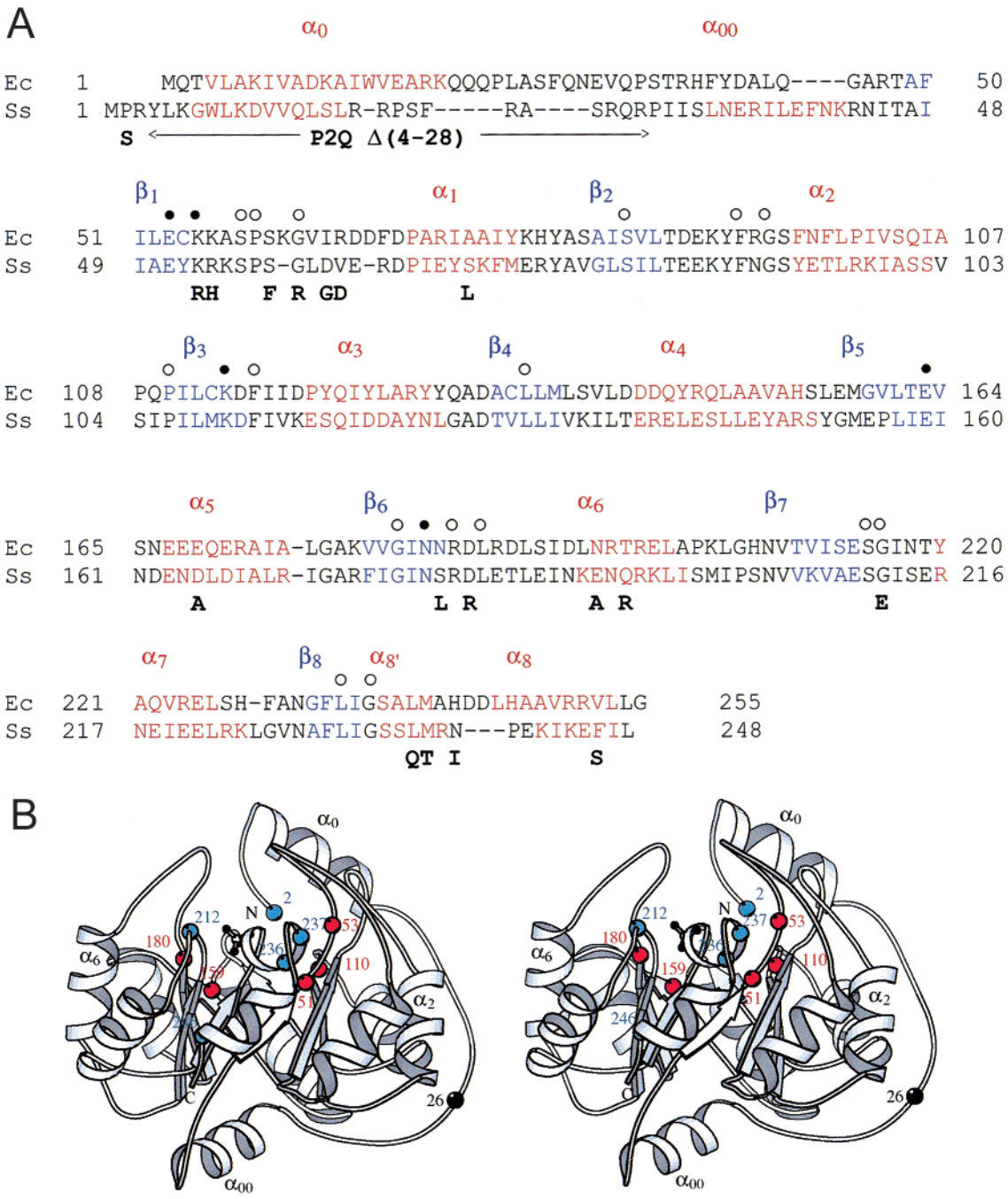

FIGURE 1: Location of substituted residues in the structure of sIGPS. (A) Structure-based sequence alignment of sIGPS (Ss) and eIGPS from *E. coli* (Ec) (*7*). Secondary structural elements are colored red for α-helices and blue for *β*-strands and labeled: (●) catalytically essential residues and (○) invariant residues. The bottom line lists residues substituted in individual variants. Δ(4−28) represents the deletion, including P2Q. Mutant P2S was isolated as a single mutant in vector pDS SS-1. The plasmid encoding the P2S change was subjected to another round of shuffling mutagenesis, and double variants P2S/L236Q and P2S/M237T were isolated. Variants S58F, G59R, S70L, and S181A/D165A were isolated from pMCY1 mutated with hydroxylamine. All other variants were isolated from pMCY1 by DNA shuffling (see Materials and Methods). (B) Ribbon diagram of sIGPS. Labeled Cα positions: red, catalytically essential residues; blue, selected sites of substituted residues in individual variants; and black, R26, the site of cleavage by trypsin. The figure was drawn using MOLSCRIPT (*39*).

Trp curve in Figure 2). The plasmids encoding P2S/L236Q, P2S/F246S, and P2S/M237T also supported maximal growth. In contrast, combining the change K53R in loop $\beta_1\alpha_1$ with the change F246S in helix α_8 gave a combination that was less active than either parent alone (data not shown). Many of these residues are quite close to each other at the top of the barrel (Figure 1B), and presumably lead to adverse interactions.

Regulation of the *trp* operon is not compromised by the particular deletion of the e*trpC* gene that was used. Therefore, the slow growth of the transformants bearing the plasmid-borne s*trpC* gene must be due to the low enzymatic activity of sIGPS leading to low levels of intracellular tryptophan. This low activity must lead to derepression of the *trp* operon. As a result, the substrate of IGPS (CdRP) accumulates in the cells and is excreted into the medium (*29*, *30*). Con-

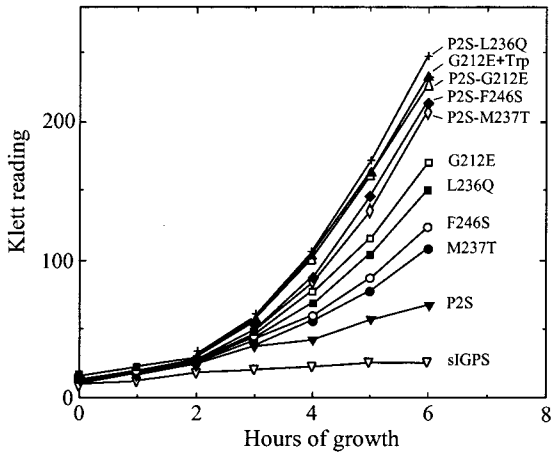

FIGURE 2: Growth curves in liquid minimal medium of the *E. coli* Δ*trpC* deletion strain transformed with plasmids encoding sIGPS or the indicated variants. G212E+Trp is the trace for the maximal growth of G212E in the presence of 20 μg of L-Trp/mL and 100 μg/mL ampicillin. Growth rates were measured by light scattering (Klett colorimeter).

versely, transformants expressing functionally improved variants of sIGPS are expected to increase the level of tryptophan and therefore will grow more rapidly. Consequently, the levels of the other enzymes of Trp biosynthesis are repressed, and the concentration of CdRP is decreased by both slower production and faster consumption. As expected, the extent of CdRP accumulation correlated inversely with the growth rates of strains with the different mutant plasmids (Table 1). Only traces of CdRP were detected after 6 h in culture filtrates of strains with plasmids P2S/L236Q, P2S/G212E, P2S/F246S, and P2S/M237T, and CdRP was not detected following overnight growth of these strains. Low to moderate levels of CdRP were observed with plasmids encoding the G212E, L236Q, F246S, and M237T variants, and high levels with plasmids encoding P2S, F53R, R54H, D183Y, and Q194R variants of sIGPS. These findings suggest that growth rate is directly related to the specific enzymatic activity of each strain's IGPS variant. In other words, different levels of protein synthesis, folding, and stability appear to make negligible contributions to growth rates.

Choice of Instructive Variants. The five single-site variants P2S, G212E, L236Q, M237T, and F246S have changes in two structurally and functionally important regions of sIGPS (cf. panels A and B of Figure 1). (a) In the N- and C-termini, P2S and F246S are disruptive substitutions that presumably increase the flexibility of the rigid structure of sIGPS by promoting fraying at the termini, and (b) in the complex phosphate binding site, the amide proton of G212 hydrogen bonds to one of the phosphate oxygens (*7*, *27*). Although this interaction might still be preserved in G212E, its negatively charged side chain should repel, or perhaps even replace, the bound phosphate. Moreover, helix $\alpha_{8'}$, which points its positive α-helical dipole at another phosphate oxygen, is anchored by both L236 and M237 to the surface of the protein. L236Q and M237Q are disruptive substitutions that are likely to destabilize helix $\alpha_{8'}$, consequently decreasing the enzyme's affinity for phosphate. We therefore chose these variants and their faster growing combinations with P2S for further studies.

Table 1: Relative Extract Specific Enzyme Activities[a]

protein[b]	relative specific activity[c] 37 °C	55 °C	80 °C[f]	growth rate[d]	concentration of accumulated CdRP[e]
sIGPS	0.2	1.5	16	+	+++
P2S	0.5	3.8	13	+	+++
M237T	0.6	2.1	(5)[g]	++	++
F246S	1.2	3.0	(6)	++	++
L236Q	0.8	3.3	(3)	++	++
G212E	1.8	6.2	22	+++	+
P2S/M237T	2.3	5.2	(7)	+++	−
P2S/F246S	2.3	5.7	(10)	+++	−
P2S/G212E	2.7	8.1	12	+++	−
P2S/L236Q	3.4	10.0	(7)	+++	−
eIGPS-PRAI	1.0	0.28	0	+++	−

[a] Cell growth and soluble cell extracts obtained as described in Materials and Methods. [b] Variants of sIGPS with the given amino acid substitutions. [c] Units per milligram of protein, normalized to the specific activity of the bifunctional enzyme eIGPS-PRAI, expressed by *E. coli* strain W3110, grown as a control culture. The buffer was 0.1 M Tris chloride (pH 7.8). [d] See Figure 2. [e] Colorimetric assay described in Materials and Methods. [f] Bovine serum albumin (0.05%) was added to samples assayed at 80 °C. [g] Parentheses indicate minimal estimate because of thermolability.

Specific Activity and Thermostability in Cell Extracts. To measure the specific enzyme activity of the proteins produced by the selected plasmids directly, each was introduced into an *E. coli* strain with the entire *trp* operon deleted and the *tna* operon inactivated [W3110 *tnaA2* Δ*trpEA2* (*18*)]. The resulting transformants were grown in liquid minimal medium containing ampicillin, to maintain plasmid stability, and excess tryptophan. For reference, the standard wild-type *E. coli* strain W3110 that produces the bifunctional enzyme eIGPS-PRAI was cultured in the absence of ampicillin and tryptophan, under otherwise identical conditions. Harvested cells from each culture were disrupted by sonication, and the centrifuged extracts that were obtained were assayed at 37 °C for both IGPS activity (*19*) and the total amount of protein. The relative concentration of sIGPS and its variants was estimated by SDS−PAGE, followed by staining with Coomassie blue. Approximately the same amount of sIGPS was present in each extract (data not shown), proving that the different variants accumulated to the same levels, due to similar protein synthesis, folding, and stability at 37 °C. As presented in Table 1, the relative specific activities at 37 °C increase roughly in proportion to the respective growth rate (Figure 2), supporting the conclusion that the selected functional property of these variants is the turnover number (k_{cat}).

The activity measurements were repeated at 55 and 80 °C to estimate the effect of temperature on activity (the net effect of increasing temperature on the gain of k_{cat} and the simultaneous loss of protein by irreversible thermal inactivation). Table 1 shows that variants P2S and G212E are about as thermostable as sIGPS, whereas the other single-site variants are much less thermostable. Again, except for P2S/G212E, the destabilizing effects of single-substitution variants are additive when combined with the effects of P2S, but all variants are much more thermostable than eIGPS-PRAI from *E. coli* (Table 1).

Enzyme Catalytic Constants. The variant proteins listed in Table 2 were purified to homogeneity to characterize their activity, flexibility, and thermostability in more detail. The corresponding genes were heterologously expressed in *E. coli*

Table 2: Enzyme Kinetic Constants of sIGPS and Temperature Dependence and Comparison to Those of Selected Variants[a]

protein[b]	T (°C)	k_{cat} (s^{-1})	K_M (μM)	K_P (μM)	k_{cat}/K_M (μM^{-1} s^{-1})
	25	0.03	0.04	0.02	0.7
sIGPS	37	0.15	0.05	0.03	3.0
	60	0.98	0.05	0.06	14.2
P2S	37	0.16	0.05	0.04	3.2
F246S	37	0.35	0.40	0.30	0.9
G212E	37	0.36	5.60	2.60	0.1
P2S/F246S	37	0.27	0.42	0.39	0.6
P2S/G212E	37	0.57	10.9	3.60	0.1
eIGPS-PRAI[c]	25	3.60	0.42	0.54	8.6

[a] With 0.05 HEPPS buffer (pH 7.5), 4 mM EDTA, or 2 mM EDTA. [b] sIGPS and variants identified in Figure 1A. [c] Bifunctional eIGPS-PRAI (*22*), 0.05 M Tris chloride (pH 7.5), and 4 mM EDTA.

strain W3110 *tna*A2 Δ*trpC hsdR2, zji-202*::Tn*10*, and the mutant proteins were purified from the soluble fraction of the cell extracts to homogeneity, using standard chromatographic techniques (data not shown). Enzyme kinetic constants were determined at 37 °C with a sensitive fluorometric assay that is based on the different fluorescence properties of the substrate CdRP and the product IGP (*9*, *31*). The buffer and assay conditions that were used were different from those used for the crude extract assays, whose results are presented in Table 1. It was shown previously that sIGPS was more active in 0.05 M HEPPS buffer than in 0.05 M Tris-HCl buffer (*7*).

The turnover number (k_{cat}) of P2S is only marginally larger than that of the parental sIGPS, but the turnover numbers of G212E and F246S are doubled. Moreover, the combination with P2S increases the turnover number of G212E 2-fold further, but the same combination decreases the turnover number of F246S somewhat. As observed in some other studies (*32*, *33*), sequence changes can improve the protein folding efficiency, compensating for the decrease in activity. As also shown in Table 2, the k_{cat} value of sIGPS increases markedly with increasing temperature, so it is about as active near its physiological temperature as eIGPS at 37 °C. In contrast to the large effect of single changes on K_M, the temperature dependence of the K_M of sIGPS is only moderate.

The most striking differences are found in the K_M values, which increase 8-fold (F246S and P2S/F246S), 100-fold (G212E), and 200-fold (P2S/G212E) (Table 2). The catalytic efficiencies (k_{cat}/K_M) of the variants decrease 3−60-fold, despite the 2−4-fold increase in the turnover number k_{cat}, and mainly due to the dramatic increases in the respective K_M values. Therefore, the data for P2S, G212E, and F246S confirm that they must have been selected for increased values of k_{cat} rather than for increased catalytic efficiency. The implication that these single-site variants are always saturated with substrate in vivo (that is, [CdRP] ≥ $10K_M$) is supported by the accumulation of CdRP in the culture filtrates (Table 1). The high levels of CdRP allow the transformants producing these variants to achieve high growth rates, even though their affinities for the substrate are greatly reduced. Since only traces of CdRP accumulate in the culture filtrates of the most rapidly growing transformants (e.g., P2S/G212E), the intracellular concentration of CdRP must be much higher than the extracellular concentration for saturation of these sIGPS variants.

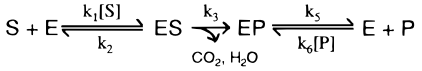

FIGURE 3: Minimal catalytic mechanism of the reaction catalyzed by sIGPS (E). S is 1-(*o*-carboxyphenylamino)-1-deoxyribulose 5-phosphate (CdRP). P is indoleglycerol phosphate (IGP). $k_4 = 0$, because decarboxylation of CdRP renders the conversion of ES → EP irreversible.

Equilibrium of IGP Binding. Having obtained several activated variants of sIGPS with increased values of k_{cat}, we now are faced with the question of how single-residue substitutions can significantly increase the turnover number of sIGPS at 37 °C. Figure 3 shows a condensed version of the catalytic mechanism of the IGPS reaction. The substrate (S = CdRP) binds in a single step to the enzyme (E); conversion of the enzyme-bound substrate (ES) to enzyme-bound product (EP) occurs in the following, irreversible step [which may actually involve several intermediates (*9*)], and product (P = IGP) is finally released in a single step by dissociation of EP. This overall mechanism suggests two alternative scenarios for the increased turnover number (k_{cat}) of the variants. (a) The irreversible conversion of ES to EP is rate-limiting in the parental enzyme, and product release is relatively fast (i.e., $k_3 \ll k_5$ in Figure 3). In this case, the measured value of $k_{cat} = k_3$. Alternatively, (b) the release of product is rate-limiting, and the chemical step is relatively fast (i.e., $k_3 \gg k_5$). In this second case, $k_{cat} = k_5$, meaning that the enzyme is "constipated". These two possibilities can be distinguished by measuring the rate constants of IGP binding to (k_6) and dissociation from (k_5) both sIGPS and a representative variant.

Kinetics of IGP Binding. We decided to focus on the variant F246S, since the substitution site is relatively far removed from the active site (Figure 1B) and yet displays significant changes in its catalytic constants (Table 2). Because decarboxylation of CdRP makes the chemical step of IGP production irreversible (i.e., $k_4 = 0$ in Figure 3), the product inhibition constant K_P is identical to the equilibrium dissociation constant K_d ($=k_5/k_6$) of the sIGPS−IGP complex. K_d was first determined independently by equilibrium binding studies. Increasing concentrations of IGP were added to a fixed, low concentration of the pure protein. The fluorescence of the mixed solutions [excited at 295 nm, where only the indole moieties of the single tryptophan residue of sIGPS (W8) and of IGP absorb, and emitted at 330 nm] exceeded that of the separately measured protein and IGP solutions, indicating that the quantum yield of W8, bound IGP, or both is increased in the protein−IGP complex. The titrations were performed in the presence and absence of protein, and the binding curve was then obtained by subtracting both the fluorescence of the protein and that of the control ligand. The thermodynamic dissociation constant K_d was calculated by fitting the data points by means of a nonlinear least-squares minimization procedure (*22*) (Figure 4) to the simple binding equilibrium given by eq 1

$$E{\cdot}IGP \underset{k_5}{\overset{k_6}{\rightleftharpoons}} E + IGP \qquad (1)$$

where $K_d = [E][IGP]/[E{\cdot}IGP] = k_5/k_6$, with [E], [IGP], and [E·IGP] being the equilibrium concentrations of the unliganded enzyme, the ligand, and the enzyme−ligand complex, respectively. A reasonable agreement was found, for both

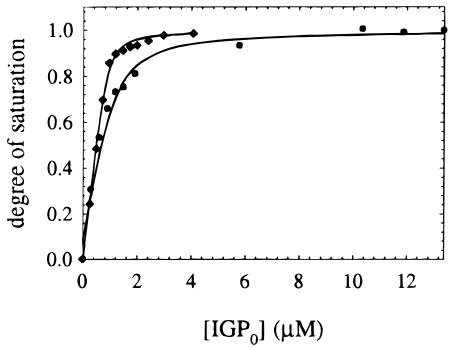

FIGURE 4: Determination of the equilibrium dissociation constant K_d of enzyme complexes with IGP. Fluorometric titration of protein with IGP at 37 °C in 0.05 M HEPPS buffer (pH 7.5) and 4 mM EDTA: (◆) sIGPS and (●) F246S. The protein concentration was 1.1 μM. The increase in fluorescence (excitation at 295 nm, emission at 330 nm) was normalized by the maximal value. (—) Best fit curves with the K_d values given in Table 3.

Table 3: Equilibrium and Rate Constants for Binding of IGP to sIGPS and the F246S Variant[a]

	equilibrium			rate[b]		
protein	K_d[c] (μM)	K_P[d] (μM)	K[e] (μM)	k_6 (μM^{-1} s^{-1})	k_5 (s^{-1})	k_{cat}[d] (s^{-1})
sIGPS	0.05	0.03	0.04	5.0	0.19	0.15
F246S	0.21	0.30	0.26	37.0	9.60	0.35

[a] Protein concentration of 1.1 μM. Buffer as in Table 2. [b] Data from Figure 5; estimated errors ± 20%. [c] Data from Figure 4. [d] Data from Table 2. [e] Average of K_d and K_P; estimated errors ± 20%.

sIGPS and the F246S variant, between the product inhibition constants K_P and the dissociation constants K_d (Table 3), confirming the increase in K_P of F246S over that of sIGPS.

The kinetics of binding of IGP to both sIGPS and the F246S variant at 37 °C was measured by using a stopped-flow instrument at a fixed concentration of protein and variable concentrations of IGP, the latter always in large excess over the concentration of binding sites. The binding process was recorded as an exponential increase in IGP fluorescence (Figure 5A). k_{obs} was determined by using eq 2

$$F_\infty - F_t = (F_\infty - F_o)\exp(-k_{obs}t) \quad (2)$$

where F_t is the time-dependent fluorescence and F_o and F_∞ are the initial and final values, respectively. The observed rate constant (k_{obs}) depends linearly on the total concentration of IGP under these conditions, as given by eq 3 (*34*):

$$k_{obs} = k_5 + k_6[\mathrm{IGP}]_{total} \quad (3)$$

Figure 5B presents the increase in k_{obs} with increasing total ligand concentration, giving k_6 as the slope of the straight line. Because the small value of k_5 cannot be determined from the ordinate intercept of the line as accurately as k_6 can be from the slope, k_5 was calculated by using eq 4

$$k_5 = k_6K \quad (4)$$

where K is the average of K_P and K_d (Table 3).

As summarized in Table 3, k_5 (0.19 s^{-1}) of wild-type sIGPS is identical, within the error limits, to its turnover number k_{cat} (0.15 s^{-1}). Thus, the turnover of wild-type sIGPS

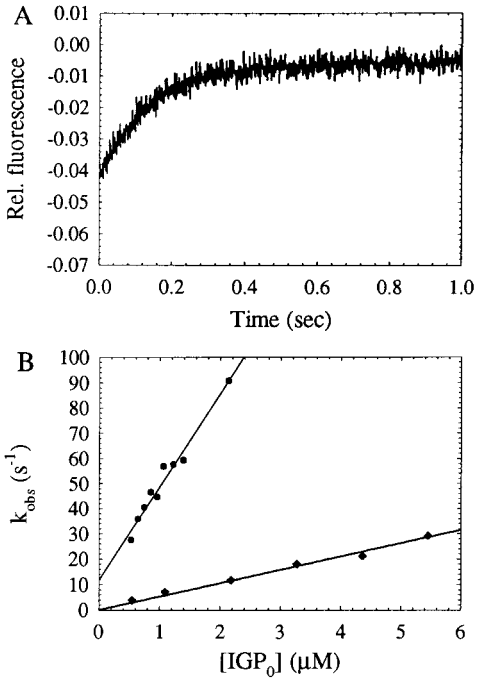

FIGURE 5: Transient kinetics of IGP binding to sIGPS and the F246 variant protein. The total protein concentration was 0.1 μM. Other conditions were as described in thr legend of Figure 4. (A) Typical transient of the monoexponential fluorescence increase. $[\mathrm{IGP}]_{total}$ = 1.1 μM. k_{obs} = 6.1 s^{-1}. (B) Dependence of k_{obs} on the total concentration of IGP. The straight lines represent fits of the rate constants for wild-type sIGPS (◆) and the F246S variant (●) to eq 3. The values of the rate constants are given in Table 3.

is limited by release of bound IG; that is, $k_3 \gg k_5 = k_{cat}$, as in scenario b. The same measurements with F246S yielded values for the product on- and off-rate constants k_6 and k_5 that were much larger than those observed for sIGPS (Figure 5B). Moreover, k_5 (9.6 s^{-1}) is about 25-fold larger than k_{cat} (0.35 s^{-1}), showing that product release no longer limits the catalytic turnover of F246S. It follows from the mechanism (Figure 3) that the chemical step (k_3 = 0.35 s^{-1}) now limits the turnover rate; that is, $k_5 \gg k_3 = k_{cat}$, as in scenario a. The parental sIGPS may have the same or a larger k_3 value, but cannot have a smaller k_3 value, because the release of product is rate-limiting ($k_3 \geq k_5 = k_{cat}$).

One possible structural explanation for the large acceleration of IGP binding and release, caused by the F246S substitution, is as follows. The active site of both eIGPS (*8*) and of sIGPS (*7*, *27*) is well-shielded from the solvent. Therefore, the binding of IGP to sIGPS must be accompanied by rapid conformational changes between closed and open states, which slow the overall processes of IGP binding and release. In keeping with this view, the equilibrium between the closed and open states of the active site is shifted significantly toward the open state in the F246S variant. Since $K_P = K_d$ for G212E and is about 9-fold larger than that of F246S (Table 2), its rate constant of IGP release (k_5, Figure 3) is presumably also larger than that of F246S (Table 3). In support of this interpretation, G212E has the same turnover number as F246S, which most likely corresponds to the value of k_3 for the parental sIGPS. It follows that the further increase in k_{cat} of P2S/G212E (0.57 s^{-1}), over that of G212E alone, reflects the additional increase in k_3 above the value of 0.35 s^{-1} of sIGPS, F246S and G212E. Put differently, substitutions P2S and G212E actually cooperate to accelerate

Table 4: Flexibility and Thermostability of sIGPS and Selected Variants and Rates of Inactivation by Trypsin and Heat and Protection against Trypsinolysis by Bound IGP

	half-life (min)		
	trypsin[b]		heat[d]
protein[a]	[IGP] = 0	[IGP] = $10K_P$[c]	[IGP] = 0
sIGPS	120	120	46
P2S	60	60	18
F246S	40	nd[e]	1
G212E	40	nd[e]	38
P2S/F246S	8	60	<0.1
P2S/G212E	15	60	19

[a] sIGPS and variants with the indicated substitutions (Figure 1A). [b] Decay of full-length protein after trypsinolysis in 0.1 M Tris acetate at pH 7.8 and 25 °C, estimated by SDS−PAGE. [c] Conditions as described in footnote b, but with the IGP concentration 10-fold larger than K_P (Table 2). [d] Decay of active enzyme in 0.05 M potassium phosphate at pH 7.5 and 86.5 °C. [e] Not determined.

both the rate of product release (k_5) and the rate of the chemical step (k_3). The effect of increasing temperature on k_{cat}, K_M, and K_P shown in Table 2 suggests that the constipation by product release, which limits the activity of the parental protein at 37 °C, is relieved at 60 °C by a similar increase in flexibility as effected by single- or double-residue replacements at 37 °C.

Protein Flexibility and Ligand Binding. Possible changes in the native-state flexibility of sIGPS and the variants were probed semiquantitatively by limited proteolysis (*35*). Trypsin cleaves solely at the R26−Q27 peptide bond of sIGPS, giving the stably folded, partially active fragment Δ(1−26)-sIGPS (B. Darimont and H. Szadkowski, unpublished experiments), similar to the deletion variant P2QΔ(4−28) reported here. R26 is located in the external loop that connects helix α_0 with helix α_{00} (Figure 1B). Moreover, the side chain of R26 points into the interior of the protein (*7*, *27*) and participates in an energetically favorable triple salt bridge cluster with R28 and D128 (on loop $\alpha_3\beta_4$). Because the peptide bond of R26 is nevertheless cleaved slowly even in wild-type sIGPS, the loop containing R26 must fluctuate dynamically to a certain extent, exposing the side chain of R26 transiently (*35*). The rate of cleavage at R26 by trypsin is therefore a qualitative measure of the mobility of loop $\alpha_0\alpha_{00}$ of sIGPS and its variants.

The purified proteins were exposed to trypsin in 0.1 M Tris buffer at pH 7.8 and 25 °C. Identical aliquots were withdrawn at different times, and the respective half-lives of the full-length protein chains were estimated from Coomassie-stained SDS−polyacrylamide gels. Table 4 shows that the half-lives of proteolysis are decreased for all variants. The most likely explanation is that the disruptive substitutions loosen indirectly loop $\alpha_0\alpha_{00}$ containing the susceptible R26−Q27 bond (Figure 1B), irrespective of their position in the structure. In support of these long-range perturbations, the effects are additive in the double-site variants, particularly in P2S/F246S. Thus, loosening both the N- and C-termini seems to increase synergistically the flexibility of a larger part of the structure of sIGPS.

To check whether this loop flexibility is also coupled to the binding of substrates and products to the active site, we repeated the trypsin digestion experiments in the presence of IGP at levels leading to 90% saturation, that is, at concentrations 10-fold larger than the respective K_P value. These concentrations of IGP did not inhibit trypsin (data not shown). Table 4 shows that bound IGP protects the most susceptible double-site variants P2S/F246S and P2S/G212E relatively efficiently. We conclude that the product IGP, and most likely also the substrate CdRP, shifts the conformational equilibrium of these variants from a flexible to a more rigid conformation that also decreases the accessibility of R27 in loop $\alpha_0\alpha_{00}$.

Protein Stability. Protein unfolding studies can reveal the loosening of protein structure by amino acid substitutions (*5*). However, attempts to unfold sIGPS with guanidinium chloride under equilibrium conditions were unsuccessful. sIGPS unfolds very slowly and aggregates strongly in the unfolding transition induced by guanidinium chloride (*7*). Therefore, the relative kinetic stability of the purified variants was assessed by measuring their rates of irreversible thermal denaturation. Because this rate is governed by the many elementary interactions that must be overcome simultaneously between the ground state and the transition state of protein unfolding, it is a biologically relevant, albeit operational, criterion of thermostability (*21*, *36*).

Table 4 confirms the relatively high thermostabilities of P2S, G212E, and P2S/G212E, and the low thermostability of F246S detected in Tris buffer (Table 1). Moreover, there is a correlation between the location of the substitution and heat sensitivity in the following sense. The α-amino group of S2 in P2S cannot form the salt bridge to E141 analogous to that of P2, because its OH group would have to point into the hydrophobic pocket. Thus, the loosened N-terminus of P2S could account for the 2-fold decrease in thermal stability. In the analogous case of tIGPS, disruption of the R2−D184 salt bridge by the substitution D184A (*21*) has only a minor effect on the rate of thermal inactivation. F246 is located close to the C-terminus of sIGPS, at the end of helix α_8 (Figure 1B). The phenyl ring of F246 is part of a multiple hydrophobic cluster, which strengthens the interaction between modules $\beta\alpha_1$ and $\beta\alpha_8$, the noncovalent closure of the $(\beta\alpha)_8$-barrel, and supports the phosphate-binding helix $\alpha_{8'}$. Substitution of the bulky, hydrophobic side chain of F246 with the small, hydrophilic side chain of serine must weaken this cluster, resulting in a less stable protein. In support of this interpretation, disruption of a salt bridge (E73−R241) that cross-links the adjacent helices α_1 and α_8 in the analogous case of tIGPS, by the substitution R241A (*21*), has a strongly destabilizing effect. These observations indicate that, at least in the IGPS fold, the closure between the $\beta\alpha_1$ and $\beta\alpha_8$ modules is the weak spot. G212 in loop $\beta_7\alpha_7$ is invariant (Figure 1A), and its amide proton is probably hydrogen-bonded to the phosphate moiety of both the substrate and the product. There is enough space in the wild-type structure to accommodate the larger side chain of glutamate, without disrupting these stabilizing interactions. As expected, no large decrease in thermal stability or resistance toward trypsinolysis (Table 4) is observed.

Consistent with these correlations, the individual destabilizing effects are additive in P2S/F246S, but not in P2S/G212E. Overall, the correlation between protein flexibility and the rate of thermal inactivation supports the idea that the dampening of fluctuations between adjacent secondary structural elements ["resilience" (*4*)], as well as the fixation

of the N- and C-termini, plays an important role in stabilizing sIGPS.

sIGPS is strongly stabilized in phosphate buffer ($t_{1/2}$ = 46 min at 87 °C; Table 4) in comparison to HEPPS buffer ($t_{1/2}$ = 4.4 min at 89 °C; *7*), presumably by the bound phosphate. This observation indicates that phosphate is a multiple electrostatic clamp between K53 (loop $\beta_1\alpha_1$), G212 (loop $\beta_7\alpha_7$), and the helix dipole of helix $\alpha_{8'}$ (Figure 1B), that is, between protein modules that are far apart in the protein sequence but adjacent in space. Thus, there is a significant correlation between the decreased affinity of the variants for both the substrate and the product (i.e., increase in K_M and K_P; Table 2) and the increase in their flexibility and heat sensitivity (Table 4).

CONCLUSIONS

The catalytic turnover of sIGPS at 37 °C is limited by the rate constant of product release, apparently because the peptide loops that obstruct the active site are not flexible enough at low temperatures. In support of this interpretation, raising the temperature also activates the parental enzyme. Because the rate constant of product release of the variant F246S is substantially increased, the actual catalytic process becomes rate-limiting. This switch is presumably achieved by loosening the complex phosphate binding site, indirectly in the case of both F246S and P2S, which are located at the C- and N-terminus, respectively. Other substitutions weaken the binding of phosphate more directly, for example, G212E by electrostatic repulsion or L236Q and M237T by unfolding of helix $\alpha_{8'}$. The simultaneous increase in turnover numbers and decrease in both substrate and product affinities as well as the increase in overall protein flexibilities explains why the pairwise combinations of single-residue changes lead to synergistic activation. However, these correlations are not a necessary consequence, but seem to be due rather to the lack of selective pressure on the joint preservation of high substrate affinity and protein thermostability. Given the restricted choice of alternative residues when only single-base pair changes occur [on average six out of 19 (*37*)], acceleration of product release seems to be the simplest way to activate the parental protein, even if it is at the cost of substrate affinity and protein stability. Since there is no necessary inverse correlation between enzyme activity and protein stability (*38*), variants with much greater activity at low temperatures might be obtained by producing multiply substituted variants and screening for those that have both high activity and thermostability. Alternatively, selection could be performed under conditions precluding accumulation of high concentrations of the enzyme's substrate.

ACKNOWLEDGMENT

We are grateful to Dr. Michael Hennig and Dr. Reinhard Sterner for constructive criticism, Virginia Horn for help with the growth experiments, and Erika Johner for preparing the manuscript.

REFERENCES

1. Jaenicke, R., and Böhm, G. (1998) *Curr. Opin. Struct. Biol. 8*, 738−748.
2. Ladenstein, R., and Antranikian, G. (1998) *Adv. Biochem. Eng. Biotechnol. 61*, 37−85.
3. Varley, P. G., and Pain, R. H. (1991) *J. Mol. Biol. 220*, 531−538.
4. Aguilar, C. F., Sanderson, I., Moracci, M., Ciaramella, M., Nucci, R., Rossi, M., and Pearl, L. H. (1997) *J. Mol. Biol. 271*, 789−802.
5. Zavodszky, P., Kardos, J., Svingor, A., and Petsko, G. A. (1998) *Proc. Natl. Acad. Sci. U.S.A. 95*, 7406−7411.
6. Kohen, A., Cannio, R., Bartolucci, S., and Klinman, J. P. (1999) *Nature 399*, 496−499.
7. Hennig, M., Darimont, B., Sterner, R., Kirschner, K., and Jansonius, J. N. (1995) *Structure 3*, 1295−1306.
8. Wilmanns, M., Priestle, J. P., Niermann, T., and Jansonius, J. N. (1992) *J. Mol. Biol. 223*, 477−507.
9. Darimont, B., Stehlin, C., Szadkowski, H., and Kirschner, K. (1998) *Protein Sci. 7*, 1221−1232.
10. Stueber, D., Matile, H., and Garotta, G. (1990) in *Immunological Methods*, pp 121−152, Academic Press, New York.
11. Stemmer, W. P. C. (1994) *Nature 370*, 389−390.
12. Stemmer, W. P. C. (1994) *Proc. Natl. Acad. Sci. U.S.A. 91*, 10747−10751.
13. Zhao, H., and Arnold, F. H. (1997) *Nucleic Acids Res. 25*, 1307−1308.
14. Davis, R. W., Botstein, D., and Roth, J. R. (1980) in *Advanced Bacterial Genetics*, p 94, Cold Spring Harbor Laboratory Press, Plainview, NY.
15. Tutino, M. L., Scarano, G., Marino, G., Sannia, G., and Cubellis, M. V. (1993) *J. Bacteriol. 175*, 299−302.
16. Vogel, H. J., and Bonner, D. M. (1956) *J. Biol. Chem. 218*, 97−106.
17. Creighton, T. E. (1968) *J. Biol. Chem. 243*, 5605−5609.
18. Schneider, W. P., Nichols, B. P., and Yanofsky, C. (1981) *Proc. Natl. Acad. Sci. U.S.A. 78*, 2169−2173.
19. Creighton, T. E., and Yanofsky, C. (1970) *Methods Enzymol. 17*, 365−380.
20. Lowry, O. H., Roseborough, N. J., Farr, A. L., and Randall, R. J. (1951) *J. Biol. Chem. 193*, 265−275.
21. Merz, A., Knöchel, T., Jansonius, J. N., and Kirschner, K. (1999) *J. Mol. Biol. 288*, 753−763.
22. Eberhard, M., Tsai-Pflugfelder, M., Bolewska, K., Hommel, U., and Kirschner, K. (1995) *Biochemistry 34*, 5419−5428.
23. Cornish-Bowden, A. (1995) *Fundamentals of enzyme kinetics*, Portland Press Ltd., London.
24. Hommel, U., Eberhard, M., and Kirschner, K. (1995) *Biochemistry 34*, 5429−5439.
25. Pace, C. N., Vajdos, F., Fee, L., Grimsley, G., and Gray, T. (1995) *Protein Sci. 4*, 2411−2423.
26. Kirschner, K., Wiskocil, R. L., Foehn, M., and Rezeau, L. (1975) *Eur. J. Biochem. 60*, 513−523.
27. Knöchel, T., Hennig, M., Merz, A., Darimont, B., Kirschner, K., and Jansonius, J. N. (1996) *J. Mol. Biol. 262*, 502−515.
28. Eberhard, M., and Kirschner, K. (1989) *FEBS Lett 245*, 219−222.
29. Doy, C. H., and Gibson, F. (1959) *Biochem. J. 72*, 586−597.
30. Smith, O. H., and Yanofsky, C. (1960) *J. Biol. Chem. 235*, 2051−2057.
31. Hankins, C. N., Largen, M., and Mills, S. E. (1975) *Anal. Biochem. 69*, 510−517.
32. Gulick, A. M., and Fahl, W. E. (1995) *Proc. Natl. Acad. Sci. U.S.A. 92*, 8140−8144.
33. Kano, H., Taguchi, S., and Momose, H. (1997) *Appl. Microbiol. Biotechnol. 47*, 46−51.
34. Bernasconi, C. F. (1976) *Relaxation Kinetics*, Academic Press, New York.
35. Hubbard, S. J., Eisenmenger, F., and Thornton, J. M. (1994) *Protein Sci. 3*, 757−768.
36. Pappenberger, G., Schurig, H., and Jaenicke, R. (1997) *J. Mol. Biol. 274*, 676−683.
37. Kuchner, O., and Arnold, F. H. (1997) *Trends Biotechnol. 15*, 523−530.
38. Giver, L., Gershenson, A., Freskgard, P. O., and Arnold, F. H. (1998) *Proc. Natl. Acad. Sci. U.S.A. 95*, 12809−12813.
39. Kraulis, P. (1991) *J. Appl. Crystallogr. 14*, 946−950.

BI992333I